Simulated Lunar Gravity Testing of VIPER Loop Heat Pipe

Ezequiel F. Medici[1]
S&K Global Solutions, Houston, TX, 77058

Jodi C. Turk[2], and Elijah R. Stewart[3]
NASA Marshall Space Flight Center, Huntsville, AL, 35812

Tim Page[4]
Amentum Space Exploration Division, Huntsville, AL, 35812

Jose Dobarco-Otero[5]
HX5 LLC, Houston, TX, 77058

Geronimo Quintanilla[6], Thomas B. Slusser[7], Zane W. Mittag[8], Juan M. Barragan[9], Angel Alvarez-Hernandez [10]
NASA Johnson Space Center, Houston, TX, 77058

David C. Bugby[11]
NASA Jet Propulsion Laboratory, Pasadena, CA 91109

Jimmy Hughes[12], Joshua Smay[13], and Calin Tarau[14]
Advanced Cooling Technologies, Lancaster, PA, 17601

NASA's Volatiles Investigating Polar Exploration Rover (VIPER) mission consists of a rover designed to explore the lunar south pole. One of the main challenges faced by the rover during the lunar polar exploration is the adverse thermal environment. Temperatures can fluctuate more than a 100°C between day and night; potentially dropping to −246°C in permanent shadow regions. To maintain the rover components within temperature limits, VIPER's Thermal Management System (TMS) relies heavily on Loop Heat Pipes (LHPs). To assist the design of the thermal management system, an Engineering Design Unit (EDU) LHP has been tested in several opportunities under thermal vacuum (TVAC) environment. Of particular interest was the LHP performance in lunar gravity. To that end, the EDU LHP was tested at the nominal orientation within the rover assembly, vertical, and inclined such that the gravitational component acting on the LHP evaporator and condenser was 1/6g (lunar gravity is 1/6 of Earth gravity) when compared to the vertical configuration. This paper will examine the LHP conductance as one the key parameters to assess the effect of the gravity on the LHP performance.

[1] Thermal Engineer, S&K Global Solutions, Houston TX 77058.
[2] AST Heat Transfer, NASA Marshall Space Flight Center, Huntsville, AL 35812.
[3] AST Heat Transfer, NASA Marshall Space Flight Center, Huntsville, AL 35812.
[4] Thermal Engineer, NASA Marshall Space Flight Center, Huntsville, AL 35812.
[5] Thermal Analysis Engineer, HX5, Houston TX 77058.
[6] JSC Passive Thermal Engineer, NASA Johnson Space Center, Houston TX 77058.
[7] VIPER Thermal Model Coordinator, NASA Johnson Space Center, Houston TX 77058.
[8] Thermal Control System Project Manager, NASA Johnson Space Center, Houston TX 77058.
[9] VIPER Cross Cutting Integration Manager, NASA Johnson Space Center, Houston TX 77058.
[10] JSC Passive Thermal Technical Discipline Lead, NASA Johnson Space Center, Houston TX 77058.
[11] Technologist, Advanced Thermal Concepts and Analysis, NASA Jet Propulsion Laboratory, Pasadena, CA 91109.
[12] Lead Engineer, Orbital & Space Systems Product Development, 1046 New Holland Avenue Lancaster, PA 17601.
[13] Product Development Engineer, Orbital & Space Systems, 1046 New Holland Avenue Lancaster, PA 17601.
[14] Principal Engineer, Research & Development, 1046 New Holland Avenue Lancaster, PA 17601.

Acronyms and Nomenclature

CC = compensation chamber
CCHP = constant conductance heat pipe
EDU = engineering design unit
LHP = loop heat pipe
MLI = multi layer insulation
PID = proportional integral derivative
TCV = thermal control valve
TMS = thermal management system
TVAC = thermal vacuum
VIPER = volatiles investigating polar exploration rover

I. Introduction

NASA's Volatiles Investigating Polar Exploration Rover (VIPER) rover was designed to prospect for resources in the harsh thermal environment of the lunar south pole[1] where temperatures can be as low as −246°C in the permanent shadow regions. Consequently, VIPER's Thermal Management System (TMS) must be able to keep subcomponents within their operation and survival temperature limits, which is much narrower than the environmental temperature range. VIPER relies on four Loop Heat Pipes (LHPs)[2,3] to transport the waste heat generated by the electronics to the radiators where the heat is eventually dissipated to space. Yet for cold operations, those LHP must be able to stop working, or at least be able to reduce their heat transport capacity significantly (also referred to as shut down) to preserve heat and be able to survive lunar nights or traverse through permanent shadow regions of the Moon. From these basic requirements, it can be drawn that a comprehensive understanding of the relationship between the LHP heat transport capacity, the dissipated thermal load, and the rover boundary conditions is needed.

VIPER's TMS is much more complex than just four LHPs. VIPER's TMS consists of several constant conductance heat pipes, thermostats, thermosyphons, thermal straps, multi-layer insulation (MLI) blankets, and isolators. The full description of the rover thermal architecture was explained by Smay et al.[4], Alvarez-Hernadez et al.[5], and Mcbryan et al.[6]. However, to quantify the LHPs heat transport capacity under a broad range of dissipated thermal loads and the rover boundary conditions, a Thermal Vacuum (TVAC) test of a single LHP was carried out. The test article LHP was manufactured using the same specifications of the flight hardware. An exception to this was the tilt of the evaporator and condenser to have a gravitational component similar to the Moon's gravity. This change affected the liquid and vapor line's geometry by adding an additional bend (Figure 1). The length of the vapor and liquid lines remained the same as in the flight hardware. In addition to the heat transport capacity, the TVAC test was used to assess the LHP startup and hot shutdown under a Moon-like environment.

II. Test Article Configuration

The tested TMS consisted of three main thermal components: a heat spreader, a loop heat pipe (LHP), and a radiator/condenser (Figure 2). The heat spreader had 8 internal constant conductance heat pipes (CCHPs) filled with 42.9g of ammonia. The LHP consisted of an evaporator, a compensation chamber (CC), a thermal control valve (TCV), a serpentine condenser, and the metal tubes that interconnected all these subcomponents. The LHP was filled with 209.4g of propylene. The radiator consisted of a single 0.066 inches (1.67 mm) thick aluminum sheet with its top surface painted black. The TCV that is reasonably described by Walker et al.[7] (along with its first-time integration with an LHP) consists of a single inlet and two outlets that is consistent with the "splitter" configuration as opposed to a "merger´ configuration. Depending on the TCV body temperature, the valve will actuate in a continuous fashion (not on/off) between the two outlets. The TCVs used here are open 100 percent to either outlet at −10°C (referred to as fully closed) and +10°C (referred to as fully open) respectively. A fully closed TCV diverts the propylene vapor flow coming from the evaporator into the compensation chamber through the TCV bypass line. A fully open TCV allows the propylene vapor coming from the evaporator to flow directly into the radiator. A partially open TCV allows vapor to be partially diverted into the compensation and into the radiator. The partially open TCV can also allow backward flow of vapor from the CC into the radiator.

The LHP evaporator and the condenser, were tilted in the in-plane component such the Earth's gravity was 1/6 g along its main axis to match the lunar gravity. The TMS baseline vertically oriented components, such as the heat spreader, CC, LHP evaporator, etc., were tilted by 9.5° from the horizontal line (80.5° from the vertical line) since $\sin(9.5°)/\sin(90°) = 1/6$. The radiator and the serpentine baseline orientation is at 15° from the horizontal line and were thus tilted to 2.5° from the horizontal line, $\sin(2.5°)/\sin(15°) = 1/6$. The elevation difference between the CC and the

serpentine was also reduced to approximately 1/6 the height, 2.15 inches (54.61 mm). These orientation changes from the baseline TMS allowed for lunar equivalent gravity heads in terms of liquid return and transport. To achieve the angles and distances, it required the LHP tubes to be bent somewhere in the middle between the heat spreader and the serpentine. Figure 1 shows a schematic diagram depicting the final TMS in the 1/6 gravity orientation. Figure 3, Left, shows the TMS after bending the LHP tubes resting over a support structure that was designed and built specially for this test. The contact points between the TMS and the support structure where isolated using Ultem isolators.

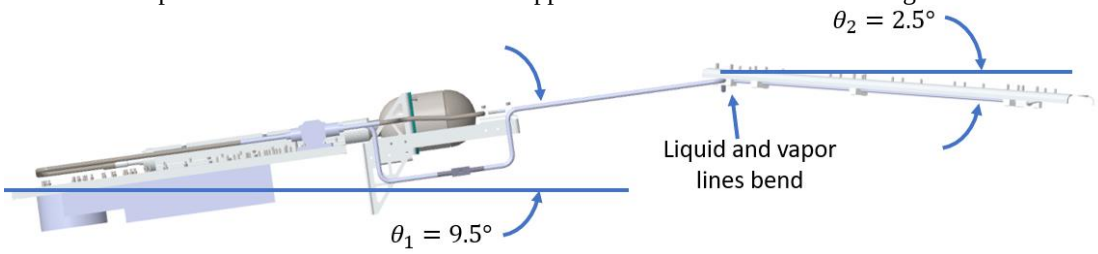

Figure 1. Tested thermal management system side view showing the tilt angles.

The test article was instrumented with three aluminum mass simulators, also acting as heater blocks simulating electronics components, attached to the heat spreader of 9.9 kg, 2.2kg, and 0.7kg respectively; 81 data thermocouples, 11 control thermocouples, and 38 heaters. The integration of these subcomponents was organized along three main actions:

- Fastening the mass simulators, with their eGraf HT-1210 interface material, to the heat spreader.
- Attaching thermocouples and heaters:
  - The measuring junction were taped using aluminum tape. All thermocouples had a strain relief loop made on the thermocouple wire adjacent to the thermocouple measuring junction.
  - Kapton heaters mounted on flat surfaces were adhered using PSA tape or epoxy. Kapton helicoidal heaters mounted on tubing were clamped and covered with aluminum tape.
  - Installation of the MLI. The MLI blankets covering the back side of the radiator were installed first. Next, the MLI blankets covering the mass simulators and the evaporator sides of the heat spreader were installed. Finally, several MLI blankets were used to provide a second layer of isolation to the evaporator and mass simulator side of the heat spreader, and to cover LHP lines, Figure 3, Right.

The thermal vacuum test lasted for two weeks, and it was conducted in a vacuum chamber that was kept at ~-170°C and $1e^{-6}$ Torr (133.32 Pa).

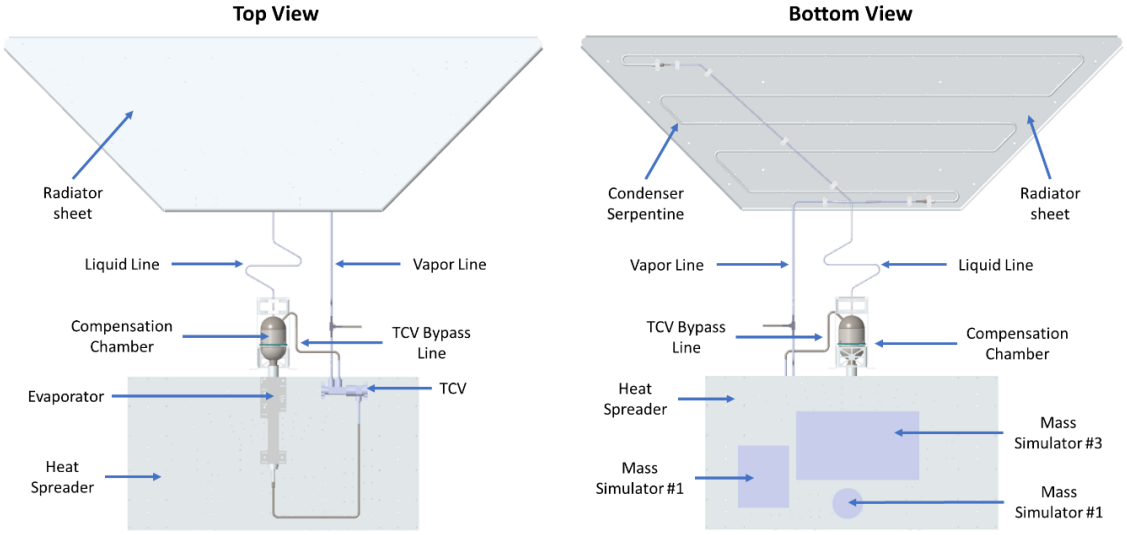

Figure 2. Left: Tested thermal management system top view showing the LHP evaporator-CC-TCV assembly. Right: Tested thermal management system bottom view showing the LHP mass simulators and condenser serpentine.

Figure 3. Left: top view of the TMS test article without MLI. Right: TMS test article with MLI.

III. Instrumentation

The TMS test article was instrumented with 81 data thermocouples, 11 control thermocouples, and 38 Kapton heaters. Table 1 summarizes the quantity and locations of the heaters and thermocouples. For a detailed location of the instrumentation please refer to the drawings shown in the Appendix. Thermocouples are classified depending on their purpose as either a data thermocouple, when used for temperature monitoring only, or as a control thermocouple, when used as reference temperature for PID control.

Table 1. Summary of the total number of heaters and thermocouples per each section of the TMS.

Compoent	Thermocouples		Heaters	
	Data	Control	Quantity	Zones
Heat Spreader	20	4	12	4
LHP Evaporator	5			
LHP Compensation Chamber	5	2	2	2
LHP TCV	4	1	1	1
LHP Serpentine	8			
LHP Liq. and Vapor Lines	5	1	3	1
Radiator Surface	9	3	7	2
Radiator MLI	2			
Radiator Isolators	4			
Heat Spreader MLI	6			
Heat Spreader Isolators	6			
Mass Simulators	7		6	3
Total TMS	81	11	25	13

Heaters were grouped into 13 thermal control zones: three survival thermal control zones (heat spreader primary, heater spreader secondary, and radiator), three thermal control zones to simulate the wasted heat from warmbox avionics, and seven operational thermal control zones (Table 2). The radiator survival heater was sized to prevent the potential freezing of propylene during cold survival. The seven ops thermal control zones were allocated for very specific TMS operating scenarios.

1) Heat spreader temperature conditioning.
2) Startup of the heat spreader embedded CCHPs.
3) Heating the TCV.
4) LHP startup/vapor line heater.

5) LHP hot shutdown primary/compensation chamber heater.
6) LHP hot shutdown secondary (redundancy)/compensation chamber heater.
7) Radiator temperature conditioning.

Table 2. Summary of the thermal zones indicating the number of heaters per zone, the electrical circuit resistance, the control thermocouple when PID is available, and the general purpose: survival, operational, and components mass simulator.

	Thermal Zone/Component	# of Heaters in Parallel	Ref. Control Thermocouple	R [Ohm]
Survival	Heat Spreader Primary	3	TC1101	16.9
	Heat Spreader Secondary	3	TC1101	16.9
	Radiator	7	TC1303	90.1
Ops.	Heat Spreader	3	TC1102/TC1103	10.0
	Heat Spreader Startup	3	TC1104	20.9
	TCV	1	TC1203	459.4
	Vapor Line	3	TC1204	47.3
	Comp. Chamber Primary	1	TC1201	29.3
	Comp. Chamber Secondary	1	TC1202	24.9
	Radiator	7	TC1301/TC1302	8.2
Mass Sim.	Mass Simulator #1	1		65.7
	Mass Simulator #2	1		22.3
	Mass Simulator #3	4		10.3

Each thermal control zone had its own dedicated power supply, a TDK-Lambda, and a power control system. The power control system could be used in at least three different modes:

1) Constant power mode, no temperature feedback control.
2) Setting on/off temperature set points, simulating a mechanical thermostat control.
3) PID temperature control. When PID temperature control feedback loop was available, a control thermocouple was designated as the reference temperature (Table 2).

Recorded data included temperatures from the data thermocouples (readings from control thermocouple were not recorded), voltage and current for each thermal control zone, chamber shroud temperature, and chamber pressure. Data were recorded at 1 Hz, although a 0.1 Hz was used for the data analysis. In addition to the automatically recorded data, a local log file was updated regularly with the voltage and current readings from each thermal control zone, time when changes to the set points were made, and time when a particular event of interest took place.

IV. Steady State LHP Performance

Steady state LHP performance was tested at 40W, 60W, 80W, 110W, 200W, and 254W constant thermal loads, which were applied to the evaporator-heat spreader assembly. No thermal load was applied to the radiator during these tests. The criteria used to define steady state temperature was a fluctuation that was no more than 0.5°C within 2 hours. LHP conductance was used to quantify the LHP heat transport capacity as a function of the thermal load. LHP conductance was calculated as the ratio between the applied thermal load and the temperature gradient between the LHP evaporator and condenser, which conservatively was defined as the minimum condenser temperature and the maximum evaporator temperature. Table 3 provides an overview of the maximum temperatures at the evaporator, minimum temperatures at the radiator, thermal loads at the evaporator, and the LHP conductance for every steady state test.

From these tests, it was observed the typical LHP conductance increases as function of the applied thermal load. In other words, the LHP increases its heat transport capacity as function of applied thermal load. This known LHP heat transport capacity tendency is a desirable quality that helps maintain the evaporator, and all the subcomponents thermally linked to it, at a stable temperature. Remarkably for this LHP, the conductance increased 40-fold, from 0.5 W/°C to 20 W/°C, when the applied thermal load increased 6-fold, from 40 W to 254 W. A similar TVAC test was conducted with the LHP having a vertical evaporator and 15° inclination on the condenser. Under that configuration, with thermal loads of 153 W and 197 W applied to the heat spreader-evaporator assembly, the conductances were

approximately 3 W/°C and 19 W/°C respectively. These values are comparable to the 2 W/°C and 13.8 W/°C conductances obtained with the current 1/6g test article at 110 W and 200 W thermal loads respectively. The lower conductance at 1/6g when compared to the 1g is an expected LHP behavior due to lower gravitational driving force acting over the fluid.

Table 3. Summary of all the steady state temperature, thermal loads, and LHP conductance for each test set point.

Evaporator Thermal Load	40 W	60 W	80 W	110 W	200 W	254 W
Max T_evap [°C]	-4.9	-1.5	0.1	7.7	18.9	36.1
Min T_rad [°C]	-90.8	-79.1	-61.6	-46.7	4.4	23.7
P_evap [W]	40.0	60.0	80.0	110.0	200.0	254.3
G [W/K]	0.5	0.8	1.3	2.0	13.8	20.4

Since the chamber shroud temperature was maintained constant throughout the duration of the TVAC test, to study the effect of the sink temperature on the LHP performance, a thermal load was applied to the radiator. Steady state LHP performance was tested at 110 W on the evaporator-heat spreader assembly and 64 W, 106 W, and 150 W thermal loads on the radiator, which were selected to mimic different solar elevation angles or expected lunar surface environmental loads. Table 4 provides an overview of the maximum temperatures at the evaporator, minimum temperatures at the radiator, thermal load at the radiator, and the LHP conductance for every steady state test. As the thermal load on the radiator was increased, the overall LHP conductance increased as well, from 2 W/°C to 31.7 W/°C. However, that increase in LHP conductance, representative of a higher LHP heat transport capacity, does not imply that the evaporator temperature will remain constant. In fact, the evaporator temperature also increased but at much slower rate in comparison to the radiator temperature change. The evaporator temperature went from 7.7°C to 33.8°C while the radiator temperature went from −46.7°C to 30.4°C for the same increase in radiator thermal load.

Table 4. Summary of all the steady state temperature, thermal loads, and LHP conductance for each test set point when a thermal load was applied to the radiator.

Radiator Thermal Load	0 W	64 W	106 W	150 W
Max T_evap [°C]	7.7	15.9	19.7	33.8
Min T_rad [°C]	-46.7	-13.1	16.5	30.4
P_evap [W]	110.0	110.0	110.0	110.0
G [W/K]	2.0	3.8	34.3	31.7

V. Survival

In the context of TVAC testing, the term survival is referring to a set of test conditions designed to evaluate the LHP performance when its heat transport capacity is reduced to its minimum. This is achieved by allowing the evaporator-CC-TCV assembly to cool down below the TCV closing temperature set point of −10°C. When the TCV temperature is below −10°C, the flow of vapor propylene leaving the evaporator is diverted back into the CC through the TCV bypass line, shutting down the driving LHP pressure differential, and therefore preventing significant, two-phase thermal energy from escaping the LHP through the radiator. Of particular interest is the power required to maintain the heat spreader at the survival temperatures of −22.2°C, and −27.2°C. To achieve these temperature targets, all thermal loads were brought to a halt and a PID control system was used to adjust the power on the heat spreader survival heaters. Thermocouple TC1101 was used as the reference temperature for the PID control system to maintain the heat spreader assembly at the survival temperatures. The thermal load on the heat spreader survival heaters needed to maintain the −22.2°C and −27.2°C survival temperatures were 10.6 W and 10.1 W respectively. Table 5 summarizes the temperatures at the heat spreader, evaporator (maximum temperature), TCV, CC, and radiator (minimum temperature) at steady for both survival tests, as measured from thermocouples T1103, T1203, T1222, T1206, and T1219, as well as the thermal load on the heat spreader survival heaters. From these temperatures, LHP conductance was calculated again as the ratio between the applied thermal load and the temperature gradient between the LHP evaporator and condenser, which was defined again as the minimum condenser temperature and the maximum evaporator temperature. The LHP conductance is also listed in Table 5. The reduction on thermal load from 10.6 W

to 10.1 W and LHP conductance from 0.083 W/°C to 0.081 W/°C agrees with the temperature reduction across the TMS. A similar TVAC test that maintained the heat spreader at −22.2°C was conducted with the LHP having a vertical evaporator, a 15° inclination on the condenser, and no TCV. Under that configuration, the LHP did not shut down and 95.8 W was needed to maintain the −22.2°C temperature at the heat spreader.

Table 5. Summary of the temperatures, thermal load and conductance observed during survival at of −22.2°C, and −27.2°C.

Location	Heat Spreader	Evaporator Max	TCV	CC	Condenser Min.	Thermal load	G
Thermocouple	T1103	T1203	T1222	T1206	T1219		
Unit	°C	°C	°C	°C	°C	W	W/°C
Survival at -22.2 °C	-22.1	-20.7	-20.8	-20.8	-117.8	10.6	0.083
Survival at -27.2 °C	-27.1	-25.4	-25.4	-25.4	-122.6	10.1	0.081
Survival at -22.2 °C with 64W on rad.	-22.1	-20.5	-20.3	-20.5	-60.6	8.2	0.2

Another survival test was carried out by applying 64W thermal load to the radiator surface while maintaining the heat spreader reference survival temperature of −22.2°C. This test aimed to investigate the LHP performance when the sink temperature is different from the cold LN2 environment provided by the chamber shroud without needing to change the shroud temperature. The operational example of this scenario will be the radiator receiving some solar radiation post lunar night. In this case, the thermal load needed to maintain the −22.2°C reference survival heat spreader temperature was reduced to 8.2 W resulting in a LHP conductance of 0.2 W/°C. This test confirmed that adding heat to the radiator will not compromise the LHP stability by driving the temperatures above the TCV closing temperature of −10°C.

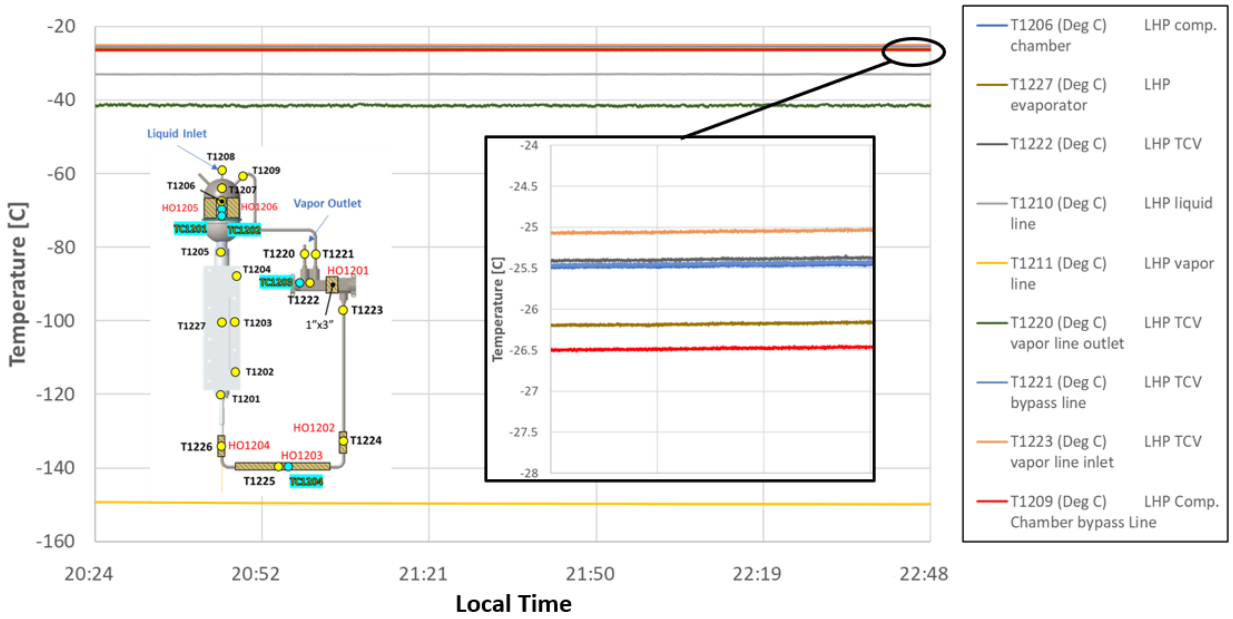

Figure 4. Temperature distribution along the evaporator-CC-TCV assembly during survival test at −22.5°C on the heat spreader.

It was also observed that at these steady state survival temperatures, the LHP flow went in reverse as indicated by the temperature readings from the thermocouples located on LHP liquid and vapor lines, T1210 and T1211 respectively. During survival testing, the liquid line thermocouple reached steady state at a temperature 100°C warmer than the temperature registered by the vapor line thermocouple. While this observation fits into the definition of reverse flow, further examination of the temperature distribution around the TCV might portray a slightly different story. Using the survival test at −22.2°C on the heater spreader as the baseline case of study, the coldest temperature

on TCV was registered at the vapor outlet thermocouple, T1220, which is consistent with a reverse flow of cold liquid propylene reaching the TCV from the condenser (Figure 4). However, this cold front does not propagate further inside the TCV nor the evaporator, as seen in thermocouples T1221, T1222, T1223, and T1227 which remained at approximately −25.5°C. The only thermocouple registering a lower temperature was T1209, −26.5°C, located at the compensation chamber end of the TCV bypass line. This could indicate that a small leakage on the TCV allowed the reverse flow to potentially go through the CC. The consequence of the reverse is a non-zero heat leak from the evaporator-heat spreader assembly in addition to the heat leaks through the MLIs and isolators. The reported thermal loads and conductance in Table 5 include all three forms of heat leaks.

VI. LHP Startup

The LHP startup from steady state survival to normal ops. was tested several times. The LHP startup test began by simultaneously applying 40 W on the mass simulator #3 heaters, 40 W on the heat spreader heaters with on/off temperature set point of −15°C/−10°C, and 40 W on the heat spreader startup heaters with on/off temperature set point of 0°C/−5°C. The 40 W thermal load of the mass simulator #3 was maintained throughout the duration of the startup test. The initial condition of the LHP startup test was heat spreader at steady state survival temperature of −22.2°C (measured at the temperature control point, TC1101; Figure 5). At the beginning of the test, the temperature of the TMS rose steadily until the heat spreader heater thermocouple (TC1103) reached its off temperature set point of −10°C. Then, the temperature of the TMS continued to rise, but at a slower rate until the heat spreader startup heater thermocouple (TC1104) reached its off temperature set point of 0°C. From this point forward, the TMS temperature rise was driven only by the thermal load of the mass simulator #3 heaters. Still, the LHP was in reverse flow mode as described in Section V Survival. Once the TCV reached the fully open temperature of 10°C, that marked the beginning of the LHP flow changing back into forward flow. The beginning of the flow switch can be observed at the liquid line thermocouple, T1210, where the temperature no longer increases but rather sharply decreases. This LHP flow change is not instant and while the flow was switching, the TMS temperature continued to rise until approximately 16.4°C. At the point, the LHP reached its fully forward flow and the TMS temperature started to decrease. Notice that when the LHP is in fully forward flow, the vapor line thermocouple suddenly jumped in temperature, tracking now the temperature of the evaporator-heat spreader assembly. The whole LHP startup process took approximately 4 hours.

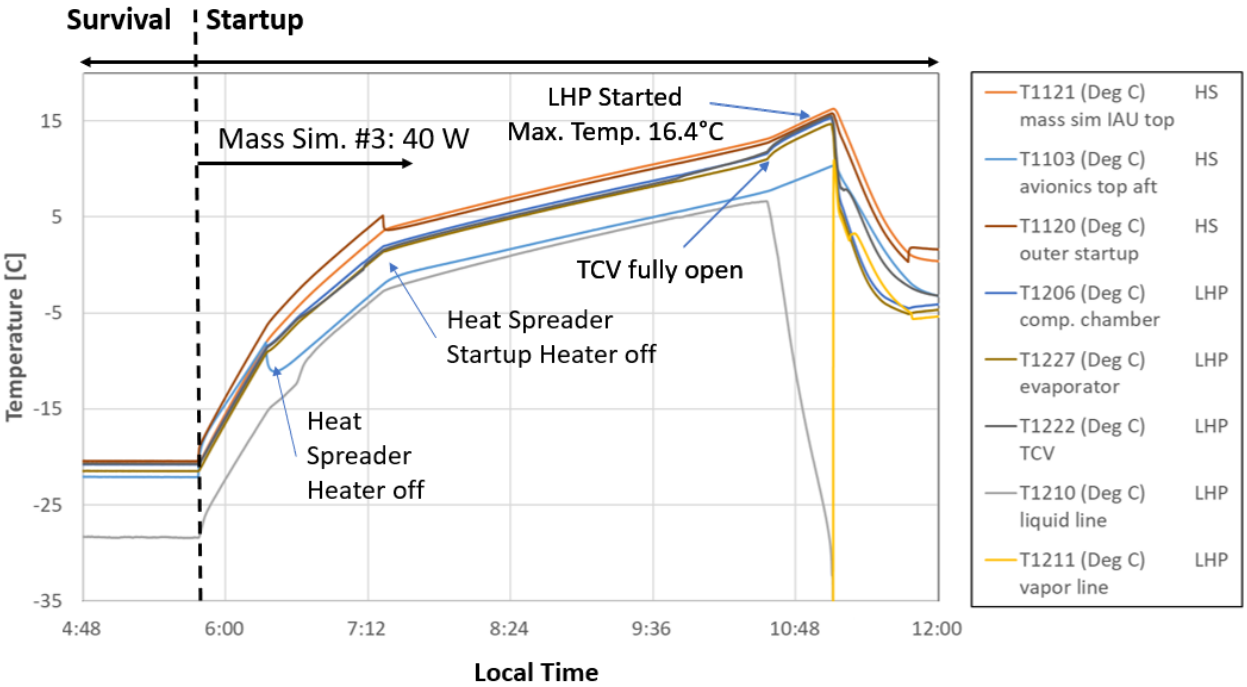

Figure 5. LHP startup thermal response from survival to normal ops. with temperature dependent thermal load. T1210 (LHP liquid lines) rapidly decreasing in temperature while T1211 (LHP vapor line) rapidly increasing in temperature is indicative of a sudden propylene flow circulation switch from reverse to forward flow.

VII. LHP Hot Shutdown

A test was conducted where thermal loads were simultaneously applied to the LHP evaporator and compensation chamber. By applying heat to the compensation chamber, and making it the hottest segment of the LHP, it forces a condition where vapor can only exist at the compensation chamber while the remaining sections of the LHP are flooded with liquid, including the evaporator, effectively shutting down the LHP. This heating strategy, called hot LHP shutdown, is used to reduce the LHP conductance and prevent heat from the heat spreader being dissipated at the condenser. The difference between hot LHP shut down and the survival LHP shutdown explained earlier, is:

- Survival LHP shutdown is a passive temperature control with predefined temperature set points.
- Hot LHP shutdown is an active temperature control where the temperature set point can be controlled by adjusting the thermal load on the CC and the evaporator-heat spreader assembly.

The initial condition for the hot LHP shut down test was baseline LHP operation, with 40 W thermal load applied to heaters located on the mass simulator #3. This thermal load resulted on an evaporator-CC-heat spreader assembly temperature around 0°C and a temperature of the liquid returning from the radiator of approximately −63°C (Figure 6). The hot LHP shut down was started by maintaining the 40 W on the mass simulator #3 heaters, adding 15 W on the mass simulator #1 heater, 45 W on the heat spreader heaters with on/off temperature set point of −35°C/40°C, and 36 W on the compensation chamber heaters with on/off temperature set point of 45°C/50°C. This complex heating choreography is representative of the combined mission plan electronic waste heat, heating control scheme, and allowable flight temperature limits, which are beyond the scope of this article. Previously, during early mission engineering design unit testing, a similar hot LHP shutdown tests have been proven successful, although using a much simpler heating choreography.

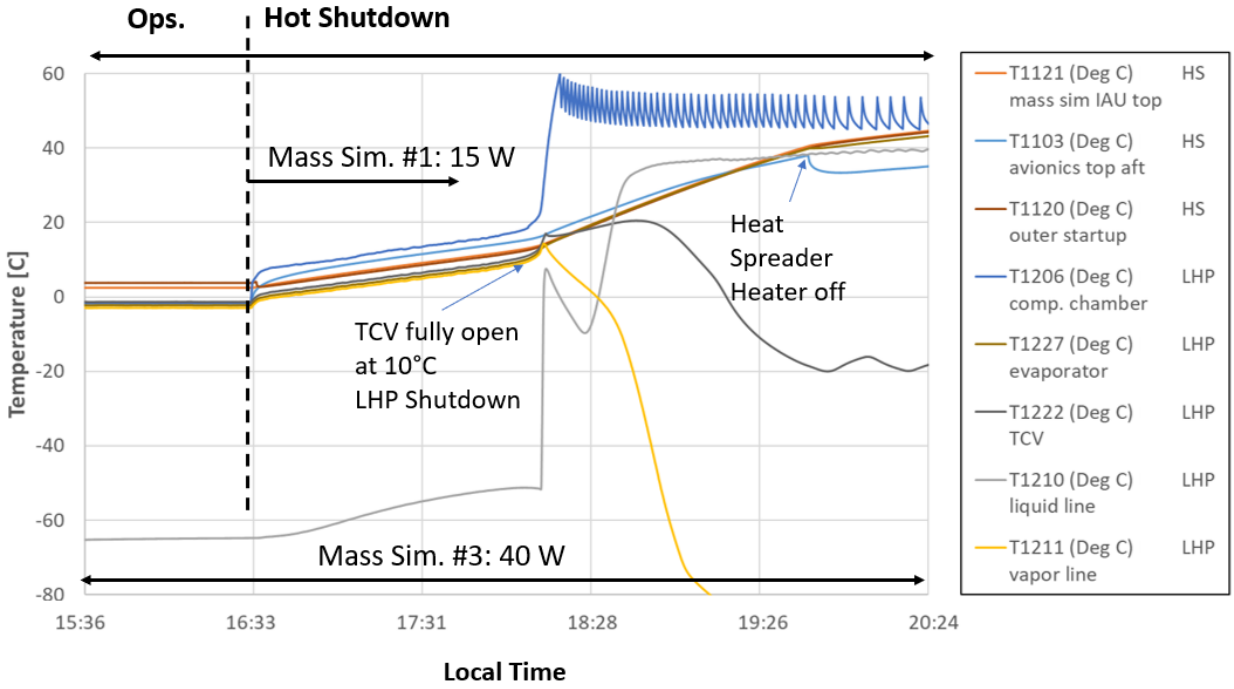

Figure 6. LHP hot shutdown thermal response from normal ops. with evaporator-CC-TCV assembly initial temperature condition around 0°C. The CC heater was turned on at 16:33 marking the beginning of the hot shutdown.

In general, the thermofluidic dynamics of hot LHP shutdown consist of a delicate balance of latent heat and partial vapor pressures. In the case of test article described here, the dynamics is even more complicated due to the presence of the TCV which can alter the partial pressure balance within the LHP. Yet, in general macroscopic terms, the hot LHP shutdown can be explained based on the observed temperature trends. At the beginning, once the heaters were enabled, the evaporator-CC-TCV assembly temperature started to rise steadily until the TCV reached 10°C (T1222). During this time, and since the TCV was partially open, the heat from CC heater generated vapor that flowed backwards through the bypass line into the TCV and to the radiator through the vapor line. This vapor leaving the CC

caused heaters not able to raise the temperature of the CC high enough to shut down the LHP flow, only a few degrees above the evaporator temperature. When the TCV body temperature reached 10°C, vapor was no longer able to flow from the CC into the radiator due to the TCV being fully open and the bypass line closed. At this point the compensation chamber temperature (T1206) increased sharply. The compensation chamber temperature was then controlled between the on/off temperature set points of 45°C/50°C. Meanwhile, the temperature of the evaporator-heat spreader assembly was still rising, the vapor line temperature started to decrease, and the liquid line temperature sharply increased, indicating reverse LHP flow, effectively shutting down the LHP. From this point forward, the temperature of the evaporator-heat spreader assembly continued to increase until the heat spreader temperature reached the off set point of 40°C. The whole hot LHP shut down prosses took approximately 2 hours.

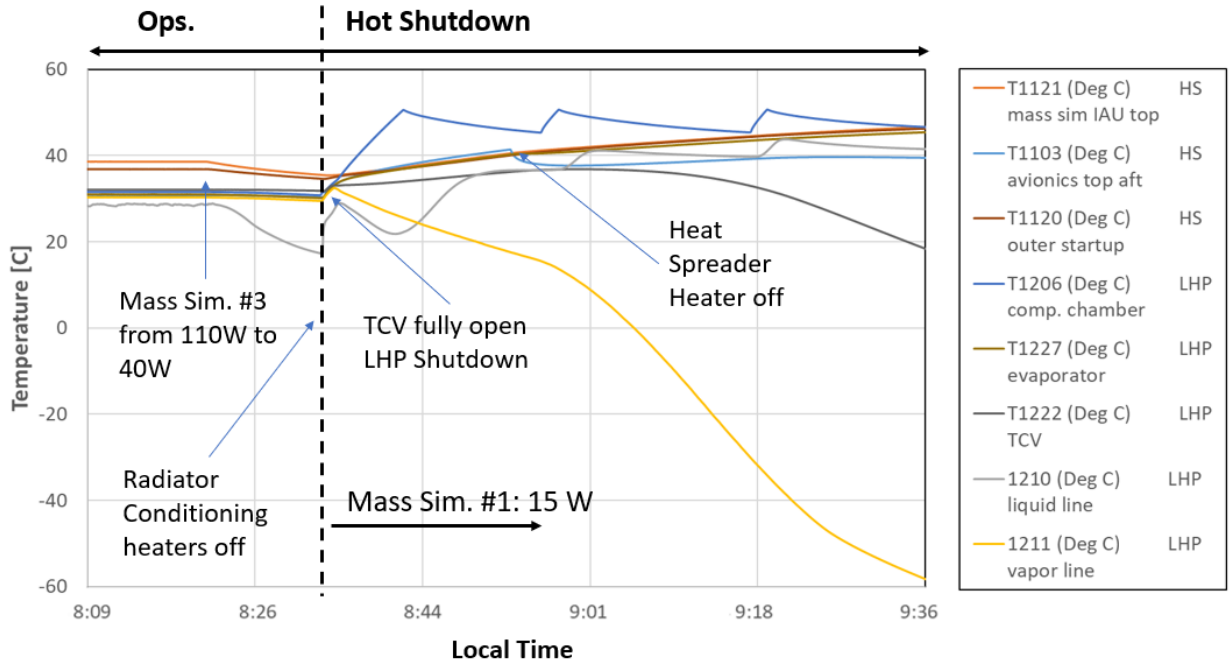

Figure 7. LHP hot shutdown thermal response from normal ops. with evaporator-CC-TCV assembly initial temperature condition around 35°C. The beginning of the hot shutdown was triggered by powering on the CC heater.

Another hot LHP shutdown test was carried out with different initial conditions where the TCV body temperature was already above 10°C (Figure 7). To achieve this initial condition, 110 W thermal load was applied to the evaporator-heat spreader assembly through heaters located on the mass simulator #3 and 150 W thermal load was applied to the radiator through radiator conditioning heaters. This thermal load configuration drove the temperature of the evaporator-heat spreader assembly to approximately 35°C. The hot LHP shut down was started by dropping the thermal load on the mass simulator #3 to 40 W, stopping the thermal load on the radiator conditioning heaters and adding 15 W on the mass simulator #1 heater, 45 W on the heat spreader heaters with on/off temperature set point of 35°C/40°C, and 36 W on the compensation chamber heaters with on/off temperature set point of 45°C/50°C. Since the TCV body temperature was already above 10°C before the beginning of the test and there was no vapor flow thought the TCV bypass line, the compensation chamber temperature started to rise sharply after the compensation chamber heater was enable. In parallel to the CC temperature rise, the vapor line temperature started to decrease and the liquid line temperature sharply increased, indicating reverse LHP flow, effectively shutting down the LHP again. In this second test the LHP shut down was almost instant, confirming the effect of the TCV on the hot LHP shutdown process. Due to test time constrains, the hot LHP shutdown was only exercised four times. In all the tested cases it was observed a consistent temperature dynamic. It is worth noticing that after the CC heater was disable and the LHP evaporator became hotter than the CC, the LHP did not self-start (forward flow). The cold TCV, −20°C, (grey line in Figure 6) prevented the LHP forward flow. To start the LHP post hot shutdown, the vapor line section of the LHP connecting the evaporator with the TCV was temporally heated up using the vapor line heaters until the LHP started to operate in forward flow.

VIII. Conclusion

The TMS performance tests described in this article proved that it can operate stable under Moon-like environment for a broad range of thermal loads. These tests played an important role in defining VIPER's thermal control system, flight rules, thermal console operator training, and model correlation. Specifically for future model correlation efforts, the steady state conductance tests provided relationship between the LHP heat transport capacity as a function of the thermal load applied to the evaporator-CC-heat spreader assembly. It was also demonstrated that the heat transport was significantly reduced by incorporating a TCV into the LHP design. This effect will be also included in future model correlation efforts. The LHP startup and hot shutdown also served as important lessons defining the heating strategy that eventually become the flight rules as well as providing experience on the dynamics of the TMS for the thermal console operators. Specifically, these two tests allowed for a real-life console operator practice which could not be tested in any other condition than in this 1/6g tilt replication.

Appendix

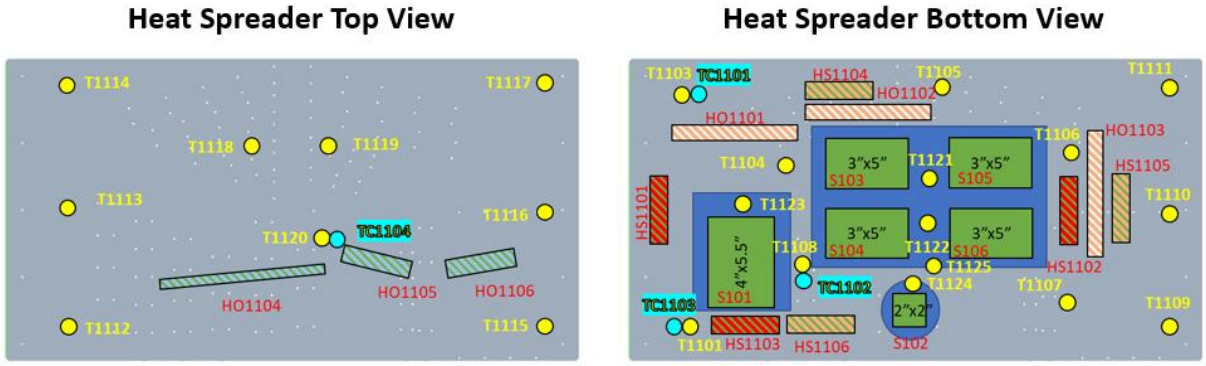

Figure 8. Heaters and thermocouples on the heat spreader and mass simulators.

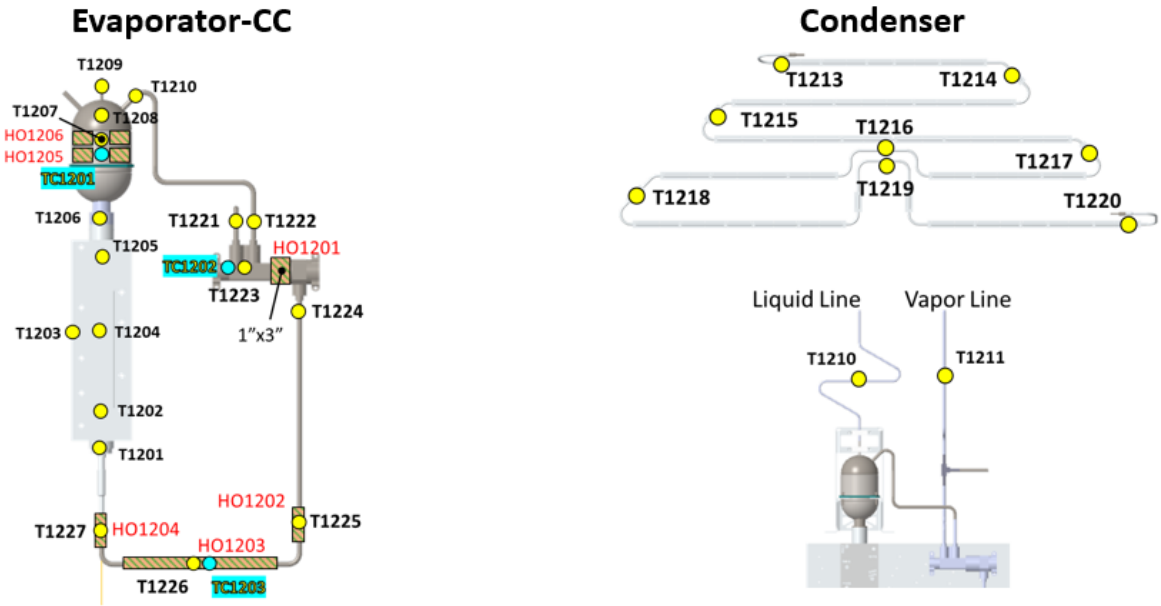

Figure 9. Heaters and thermocouples on the LHP: evaporator, CC, condenser, and liquid and vapor lines.

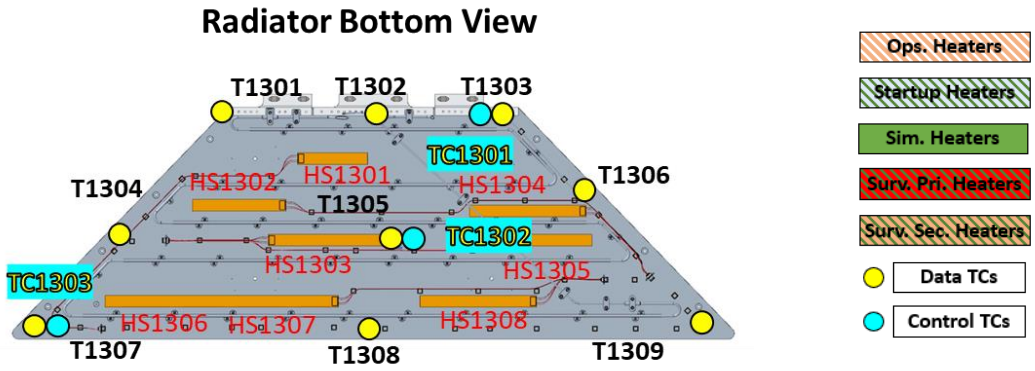

Figure 10. Heaters and thermocouples on radiator.

Acknowledgments

Any opinions, findings, and conclusions or recommendations expressed in this article are those of the authors and do not necessarily reflect the views of the National Aeronautics and Space Administration (NASA). The authors would like to thank Marshall Space Flight Center ET20 environmental test facility team, ES22 and EV34 thermal analysts for their support in carrying out the tests described in this article. The authors would also like to thank Dmitry Khrustalev whose support and contributions were crucial to the success of the test campaign.

References

[1]Colaprete, A., "Volatiles investigating polar exploration rover (VIPER)," NASA 20210015009, 2021.

[2]Ku, J., (1999). Operating characteristics of loop heat pipes. SAE transactions, 503-519.

[3]Launay S., Sartre V., and Bonjour J., "Parametric analysis of loop heat pipe operation: a literature review." *International Journal of Thermal Sciences*, Vol. 46, No. 7, 2007, pp. 621–636.

[4]Smay J., Hughes J., Spangler R., Tarau C., and Alvarez-Hernandez A. R., "Volatiles Investigating Polar Exploration Rover (VIPER) Thermal Management System (TMS) Design, Development, and Testing," *53rd International Conference on Environmental Systems*, Louisville, KY, 2024.

[5]Alvarez-Hernandez A. R., Bugby D. C., Médici E. F., Dobarco-Otero J., Rodriguez-Ruiz J. E., Mcbryan E. R., Page T., Stewart, E. R., Turk, J. C., Tarau C., Spangler R., Smay J., and Hughes J., "VIPER Thermal Management; A Systems Overview", *54th International Conference on Environmental Systems*, Prague, Czech Republic, 2025.

[6]Mcbryan E. R., Francis P., Sobey A., "Dust Mitigation for the VIPER Mobility System", *54th International Conference on Environmental Systems*, Prague, Czech Republic, 2025.

[7]Walker K. L., Hartenstine J. R., Tarau C., and Anderson W., G., "Ammonia and Propylene Loop Heat Pipes with Thermal Control Valves for Variable Thermal Conductance," *43rd International Conference on Environmental Systems*, Vail, CO, 2013.